UHI Street Typology Based on Seasonality: A Case Study from Apeldoorn, Netherlands

[1]Mónica Pena Acosta, [1]João Santos, [1]Faridaddin Vahdatikhaki, [1]Andries G. Dorée

[1]Department of Civil Engineering and Management, University of Twente, Enschede, the Netherlands
(m.penaacosta, j.m.oliveiradossanto, f.vahdatikhaki, a.g.doree) @utwente.nl

Keywords: Urban Heat Island Effect (UHI), Data-driven modelling, Seasonality, Urban data, Street typology

Abstract:

The Urban Heat Island (UHI) phenomenon results in higher temperatures in urban areas compared to less urbanized regions. This is due to the concentration of urban infrastructure, which absorbs and then releases solar radiation. Given its significant role in exacerbating the climate crisis, the UHI phenomenon demands urgent attention. While traditional physics-based simulations for studying UHI are accurate, they require substantial resources, which limits their practical application in urban planning. Previous research by the authors highlighted the capability of data-driven models as a practical alternative for assessing UHI. Such models, however, depend on the availability of extensive high-resolution datasets. Building on this prior work, the current study explores utilizing UHI's seasonality to narrow the required data scope for effective data-driven UHI modelling. By strategically targeting data collection on specific seasons, it is possible to capture UHI's intricate and dynamic nature more efficiently. This approach involved using street-based clustering to identify common seasonal patterns in Surface UHI (SUHI) and Canopy UHI (CUHI). Findings show notable seasonal fluctuations in SUHI, especially during summer. The training of Random Forest (RF) models employed varying data set proportions: 45% for summer and spring, 65% for autumn, and 75% for winter. Despite the challenges of smaller training datasets, the models achieved high accuracies, with CUHI models attaining an R^2 of 0.85 and SUHI models an R^2 of 0.74. These outcomes highlight the efficacy of strategic data collection, indicating its potential to enhance urban heat resilience and mitigate UHI effects.

1. Introduction

In recent years, escalating climate crises have led to increasingly unpredictable weather patterns in urban areas. In 2023, Europe experienced temperatures above average for 11 months, with air temperatures peaking at around 45 °C (Copernicus, 2023). This trend has exacerbated the Urban Heat Island (UHI) effect, an urban problem that urgently needs to be addressed (Peng et al., 2012). The UHI effect, which results in higher temperatures in urban areas compared to their rural surroundings, is primarily caused by the concentration of buildings, roads, and other infrastructures (Oke, 1982). These structures absorb and re-emit solar radiation. As climate change worsens, UHI is further amplified, posing severe challenges to the liveability in cities and public health, as well as increasing energy consumption and carbon emissions (Akbari et al., 2016). The consequences of UHI are far-reaching and demand immediate attention especially as global temperatures persist in setting new records.

Over the years, researchers and experts worldwide have tried to deepen their understanding of the UHI mechanisms and formulate strategies to counter its adverse effects (Akbari et al., 2016). A significant research avenue involves physics-based approaches that try to simulate thermodynamic processes within urban areas (Jandaghian and Berardi, 2020). These high-resolution simulations, which incorporate variables like construction materials, urban layout, and local climate, provide nuanced insights into urban temperature variations (Grimmond et al., 2011). While insightful, these simulations require specialized skills and high computational resources, making their practical application challenging (Mirzaei and Haghighat, 2010). Furthermore, the static nature of these solutions often fails to adapt to the dynamic nature of UHI and unpredictable climatic conditions, hindering their effectiveness in rapidly changing urban environments.

To complicate matters, UHI is grouped mainly into two types; Canopy UHI (CUHI) and surface UHI (SUHI). CUHI refers to air temperatures above the surface and below the canopy measured by weather stations placed strategically to avoid interference from urban elements. SUHI refers to the increased warmth of urban surfaces, measured on a large scale by using thermal infrared data from remote sensors in satellites or aircraft. CUHI are directly related to human exposure, where outdoor thermal comfort is crucial, making them a significant factor in human health. However, air temperatures are captured by weather stations usually placed outside the built area. This significantly compromises the spatial resolution of the measurements, i.e., only a few measurement points per city. In contrast, SUHI is derived from satellite datasets, resulting in a higher spatial resolution but very low temporal resolution. This dichotomy creates problems in accurately assessing and responding to urban heat, which are multifaceted and have far-reaching implications (Pena Acosta et al., 2023a). For instance, strategies that reduce surface temperatures, such as reflective building materials or urban greening, can also influence air temperatures by increasing humidity and decreasing thermal comfort and overall public health.

Current research methods that investigate SUHI and CUHI with high spatial and temporal resolution are somewhat limited. Studies by Du et al. (2021), Hu et al. (2019), Peng et al. (2022), and Venter et al. (2021) highlighted the tendency to overestimate SUHI intensity, especially in comparison to CUHI, and pointed out discrepancies between satellite and ground-based observations. Sun et al. (2019) further emphasized the importance of combining both air and surface. Sheng et al. (2017) found notable differences in UHI intensity in Hangzhou, China, depending on whether air temperature or Land Surface Temperature was used for measurement. Wang et al. (2020) underscored the necessity of integrating CUHI and SUHI analyses to fully comprehend urban thermal environments. In this context, the authors previously introduced a framework for

This contribution has been peer-reviewed. The double-blind peer-review was conducted on the basis of the full paper.
https://doi.org/10.5194/isprs-annals-X-4-W5-2024-255-2024 | © Author(s) 2024. CC BY 4.0 License.

simultaneously evaluating SUHI, CUHI, and a wide range of socio-economic and morphological parameters at a micro (street) resolution (Pena Acosta et al., 2023b). Also, to reduce the data collection requirement, the authors have looked into the possibility of using street typologies, i.e., a set of representative streets that exemplify the behaviour of larger street groups (Pena Acosta et al., 2024). This research demonstrated the high potential of using street typology as a means to develop a more strategic and efficient data collection regime. However, the previous research did not consider the seasonality of UHI. It is known that the mechanisms deriving UHI can change during different seasons (Schatz and Kucharik, 2014; Zhou et al., 2013). It is hypothesized that focusing on specific seasons could optimize data collection efficiency while ensuring a comprehensive analysis of UHI mechanisms, rather than maintaining continuous monitoring of the built environment. On this premise, this paper delves into the seasonal dynamics of UHI and tries to generate insights into UHI dynamics and the development of more resilient and heat-adaptive urban environments.

This paper is organized as follows: Section 2 details the research methodology. Section 3 presents the obtained results. In Section 4, these results are discussed in the context of existing knowledge. The paper concludes with a summary of findings and directions for future research.

2. Research Methodology

The research methodology for this study is organized into four main phases. The initial stage involves an analysis of the dataset previously collected by the authors, which encompasses a diverse range of socioeconomic, morphological, and environmental features for different streets. This step includes the cleaning and structuring of data to prepare for subsequent phases. In the second phase, the seasonal analysis, which is the examination of data across various seasons to identify significant variations or patterns, is conducted. The focus is on determining how different the time series of each street per season is. Dynamic Time Warping (DTW) is used in this stage for its effectiveness in comparing and measuring the similarity between time series of varying lengths and shapes. The third stage involves a cluster analysis per season, in which each season is analysed to find common patterns and characteristics of streets, to group them into one category of typology of street per season. The last stage of this methodology encompasses a validation process, where the hypothesis that selecting a particular set of streets during a specific season can encapsulate the behaviour of the entire dataset will be tested.

2.1 The data

The authors have constructed a comprehensive dataset to investigate the complex interplay between urban elements and the UHI (Pena Acosta et al., 2022; Pena Acosta et al., 2023b). To ensure thoroughness in this paper, a concise overview of the dataset is included here.

The dataset was collected in the city of Apeldoorn, the Netherlands. Apeldoorn is the 11th largest municipality in the Netherlands, and encompasses an area of about 34,115 hectares, of which 33,986 hectares are land and 129 hectares are water bodies. It has a population of 165,611 as of 2022, and it is divided into 12 residential areas, 16 districts, and 95 neighbourhoods, housing a total of 75,979 households. Its moderate oceanic climate, coupled with a unique urban layout, renders Apeldoorn a good site for studying UHI. The dataset comprises two primary components: Publicly Available cadastral datasets, and time-dependent environmental parameters.

2.1.1 Cadastral datasets: The cadastral datasets captured critical characteristics of the built environment and socio-economic factors within Apeldoorn. These encompassed five main categories: (1) Building information: details regarding the types of buildings, land use across different areas within the city, and population density; (2) Urban morphology: attributes such as street width, height-to-width ratio (H/W), and street use percentages for bicycles, vehicles, and pedestrians: (3) Building characteristics: properties such as average height, maximum height, and standard deviation of height; (4) Spatial densities: data pertaining to the densities of buildings, vegetation, and water bodies across the city; and (5) Socio-economic parameters: Features like street materials, surface colours, land use classifications, and population counts.

2.1.2 Time-dependent environmental parameters: The time-dependent environmental parameters crucial to this study were gathered through a mobile unit developed by the researchers. This unit was built to capture geo-referenced and time-stamped air and surface temperature data. The mobile unit was equipped with a versatile sensor kit, comprising components such as a GPS rover, thermologger, display, thermal camera, and data processing unit responsible for data storage. This ensemble of sensors allowed for precise and real-time temperature measurements. The measurements were taken at a consistent interval of one second while maintaining a constant cycling speed of 8 km/h. This setup resulted in a spatial resolution of 2 meters, ensuring granularity in the collected data for both surface and air temperatures. The measurements were conducted with a frequency of three times per day, precisely at 5:30 UTC, 10:30 UTC, and 16:30 UTC. This high-frequency approach enabled the study to see the evolution of diurnal temperature patterns, from the morning to afternoon and early evening. Between the months of March and September 2021, data collection occurred twice a week, while between October 2021 and February 2022, it transitioned to once a week. The data collection campaign followed an 8 km-long route, ensuring a diverse selection of 105 streets within Apeldoorn, each characterized by distinctive urban morphology and socioeconomic parameters. This comprehensive data campaign resulted in the acquisition of a total of 137,325 temperature measurements, providing a rich dataset for the subsequent analyses and findings presented in this study.

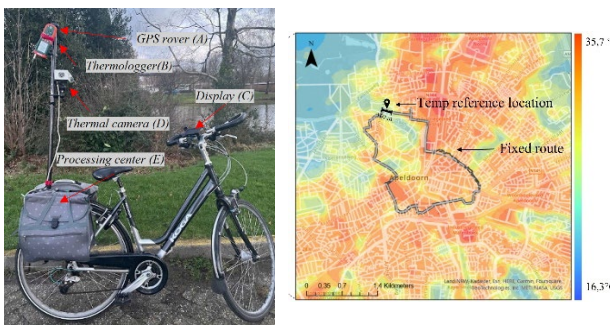

(a) Bicycle-based mobile **(b) Heatmap of Apeldoorn**

Figure 1. (a) Bicycle-based mobile urban data-gathering station; (b) Heat map of Apeldoorn, NL, illustrating the fixed route followed for the data collection campaign. The heatmap includes the temperature reference location.

2.1.3 SUHI and CUHI measurements: To calculate surface and canopy UHI, the authors took a point within the data collection area circuit to provide detailed temperature data at both the surface and canopy levels as shown in Fig. 1 (b). This was done to ensure that the street-level comparison of CUHI and SUHI could be done at the same spatio-temporal resolution. The chosen point was identified as the coolest based on average LST over the summers of 2019 to 2021 (Pena Acosta et al., 2023b).

2.2 Seasonal analysis

To investigate the seasonal dynamics of UHI patterns at a street resolution, the initial step involves plotting the time series data by season and grouping the series data into the four main primary seasons, i.e., winter (December to February), spring (March to May), summer (June to August), and autumn (September to November). From here, the next steps involve a detailed analysis of the time series data corresponding to each season. This step is crucial for identifying and understanding the specific UHI patterns that emerge during different times of the year. The focus is not only on the overall trends within each season but also on the variances and anomalies that may provide deeper insights into the UHI. This is done by implementing the Dynamic Time Warping (DTW) (Sakoe and Chiba, 1978; Witten et al., 2017). In a nutshell, the DTW algorithm enables the comparison of two time-series data that are not aligned. For example, two streets may experience the same mechanisms of UHI, but due to differing mechanisms, they may exhibit distinct patterns. By measuring the similarity between the two time series, DTW can detect and quantify the shifting patterns of UHI intensity throughout the season. This is particularly useful in the context of UHI because it enables the identification of not only the magnitude of UHI but also their temporal dynamics (similarity or divergence) observed in different streets within the same season.

2.3 Cluster analysis per season

In this step, the analysis now shifts towards optimizing data collection, by looking at the streets that best represent the mechanisms of UHI in different seasons of the year. This analysis employs the Time Series K-Means clustering (Aghabozorgi et al., 2015). This clustering technique is particularly suited for grouping time series data based on similarity in patterns, which, in this context, means streets exhibiting similar UHI mechanisms. Unlike traditional clustering methods that might not account for temporal dynamics effectively, Time Series K-Means leverages the distances calculated by the DTW to identify the natural groupings of time series data.

2.4 Validation

The last step in this methodology is the validation phase, here the hypothesis of this research is tested as follows. First, clusters for each season, identified in section 2.3, undergo a training process using a Random Forest (RF) machine learning algorithm (Roßbach, 2018). This algorithm is adept at handling complex and non-linear data, which is characteristic of UHI. Then, the RF model is incrementally trained on subsets of data per cluster, starting with 15% and scaling up to the full dataset. In each increment, the model's performance is evaluated. Clusters that demonstrate the highest predictive accuracy with the smallest subsets, measured by R-Squared, are selected for further analysis. Finally, these optimally performing clusters form a new, streamlined dataset used to train a new RF model. The predictive accuracy of this model, based on a reduced dataset, is then benchmarked against the original model for each season. The underlying hypothesis being tested is that the streamlined dataset will have a predictive performance that is on par with that of the original dataset. In other words, the reduced dataset can capture the mechanism of each season. If this hypothesis holds, it suggests that a smaller, more focused dataset can indeed capture the complex dynamics of UHI effectively.

3. Results

3.1 Seasonal analysis

Fig. 2 illustrates the patterns of the UHI for both CUHI and SUHI across the seasons in the city of Apeldoorn. The plots demonstrate the seasonal variability of heat intensity, revealing the fluctuations of UHI throughout the year. The similarities between the streets in terms of both CUHI and SUHI are quantified over the year using DTW distances, as explained in Section 2.3. This visual and statistical analysis has revealed elevated intensities during the summer and reduced intensities in the winter months, consistent with the expected patterns of temperature fluctuation. The SUHI time series plots for each season exhibit greater variability compared to the CUHI plots.
Regarding the average DTW distances, CUHI consistently displayed a lower DTW score compared to SUHI. This indicates that the CUHI time series are more similar to each other, as the cumulative distance between corresponding points in the two series, after alignment, is smaller. This suggests that the overall patterns of CUHI are more closely matched. In spring, the average DTW distance score for CUHI is 5.75, while for SUHI, it is 17.47, indicating that SUHI experiences approximately three times more variability. During summer, the variability widens further, CUHI has an average DTW score of 7.01, in contrast to SUHI with nearly five times more variability (DTW score of 35.21). In autumn, CUHI's DTW score is notably lower at 1.75, compared to SUHI's 12.49, suggesting about seven times more variability. Lastly, in winter, both CUHI and SUHI show a reduction in variability with scores of 1.75 and 5.54, respectively, indicating that during this period, the SUHI across all streets behaved more uniformly. However, this reduced variability was primarily observed during the months of December and January by the end of February. The increase in variability, as illustrated in Fig. 2(f), highlights a distinct shift in the SUHI patterns as the season progresses. The DTW scores demonstrated the significant seasonal effects on CUHI and SUHI, revealing a notably higher degree of variability in SUHI across identical urban infrastructures over the course of the year. These findings are of particular interest at this resolution level, as they underscore a potential discrepancy between mitigation strategies formulated on the basis of CUHI observations and those suitable for addressing SUHI.

3.2 Cluster analysis per season

Fig. 3, represents the clusters per season resulting from section 2.2. During Spring (Fig. 3 (a)), all three clusters, cluster_0, cluster_1, and cluster_2 performed with a certain degree of stability in their R^2 values across the various proportions of sampled streets. This suggests that the spring dataset has an inherent consistency, regardless of the cluster or the sample size (this result aligns with the results from the previous analysis in Section 3.1).

This contribution has been peer-reviewed. The double-blind peer-review was conducted on the basis of the full paper.
https://doi.org/10.5194/isprs-annals-X-4-W5-2024-255-2024 | © Author(s) 2024. CC BY 4.0 License.

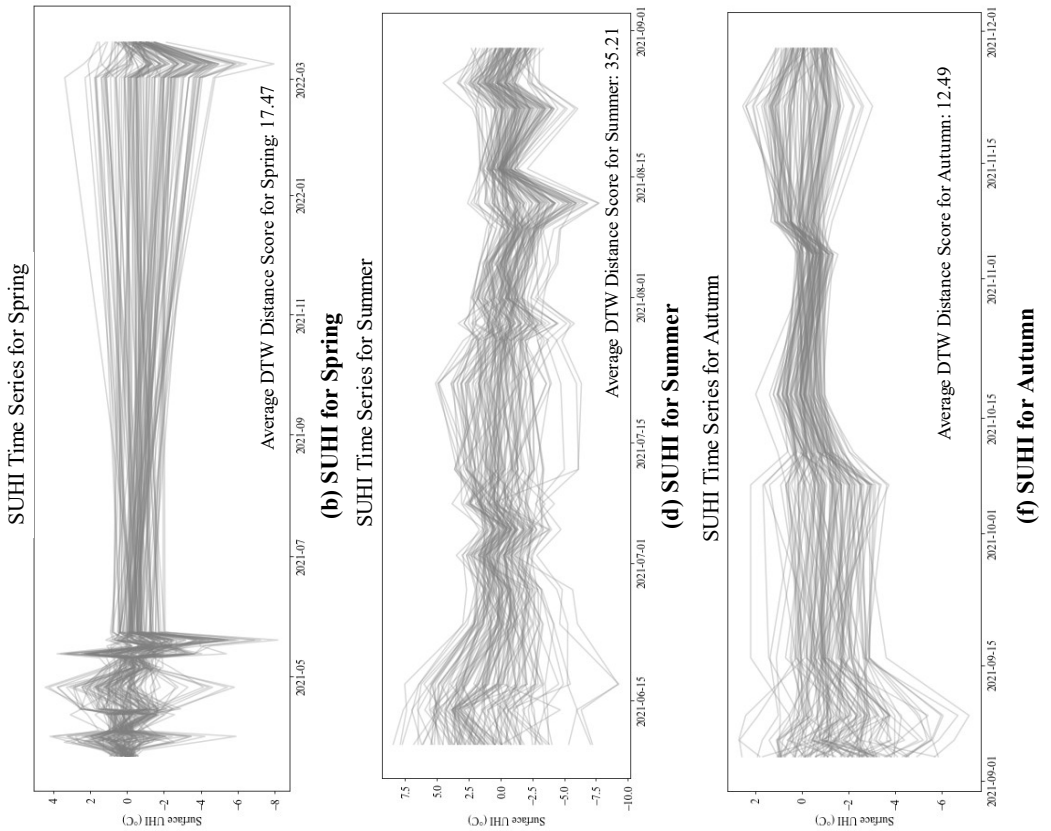
SUHI Time Series for Spring
Average DTW Distance Score for Spring: 17.47
Surface UHI (°C)
(b) SUHI for Spring
SUHI Time Series for Summer
Average DTW Distance Score for Summer: 35.21
Surface UHI (°C)
(d) SUHI for Summer
SUHI Time Series for Autumn
Average DTW Distance Score for Autumn: 12.49
Surface UHI (°C)
(f) SUHI for Autumn

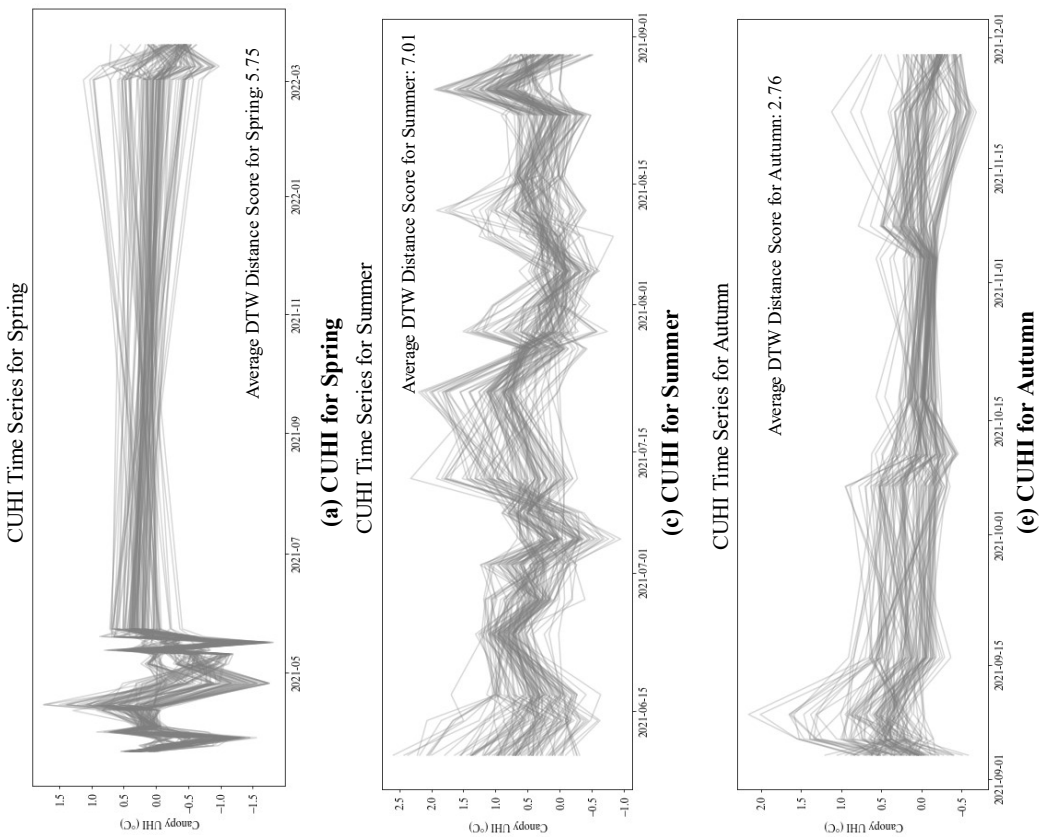
CUHI Time Series for Spring
Average DTW Distance Score for Spring: 5.75
Canopy UHI (°C)
(a) CUHI for Spring
CUHI Time Series for Summer
Average DTW Distance Score for Summer: 7.01
Canopy UHI (°C)
(c) CUHI for Summer
CUHI Time Series for Autumn
Average DTW Distance Score for Autumn: 2.76
Canopy UHI (°C)
(e) CUHI for Autumn

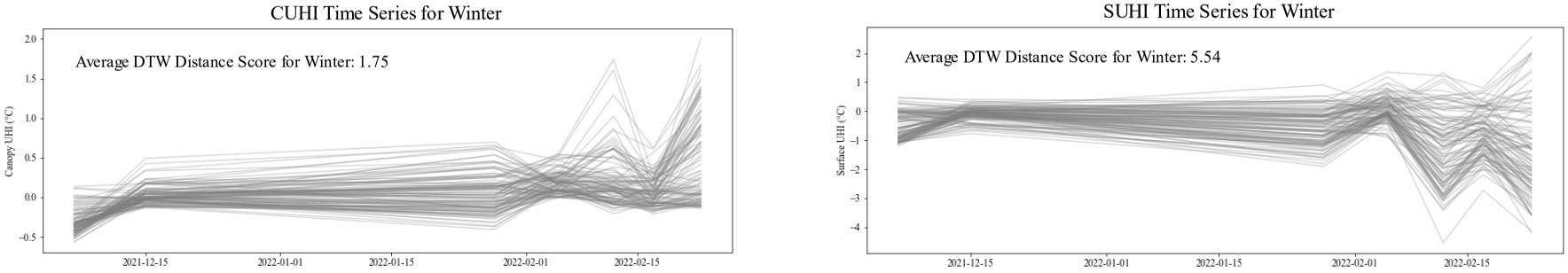

(g) CUHI for Winter **(f) SUHI for Winter**

Figure 2. Time Series representation of Canopy, and Surface UHI by season.

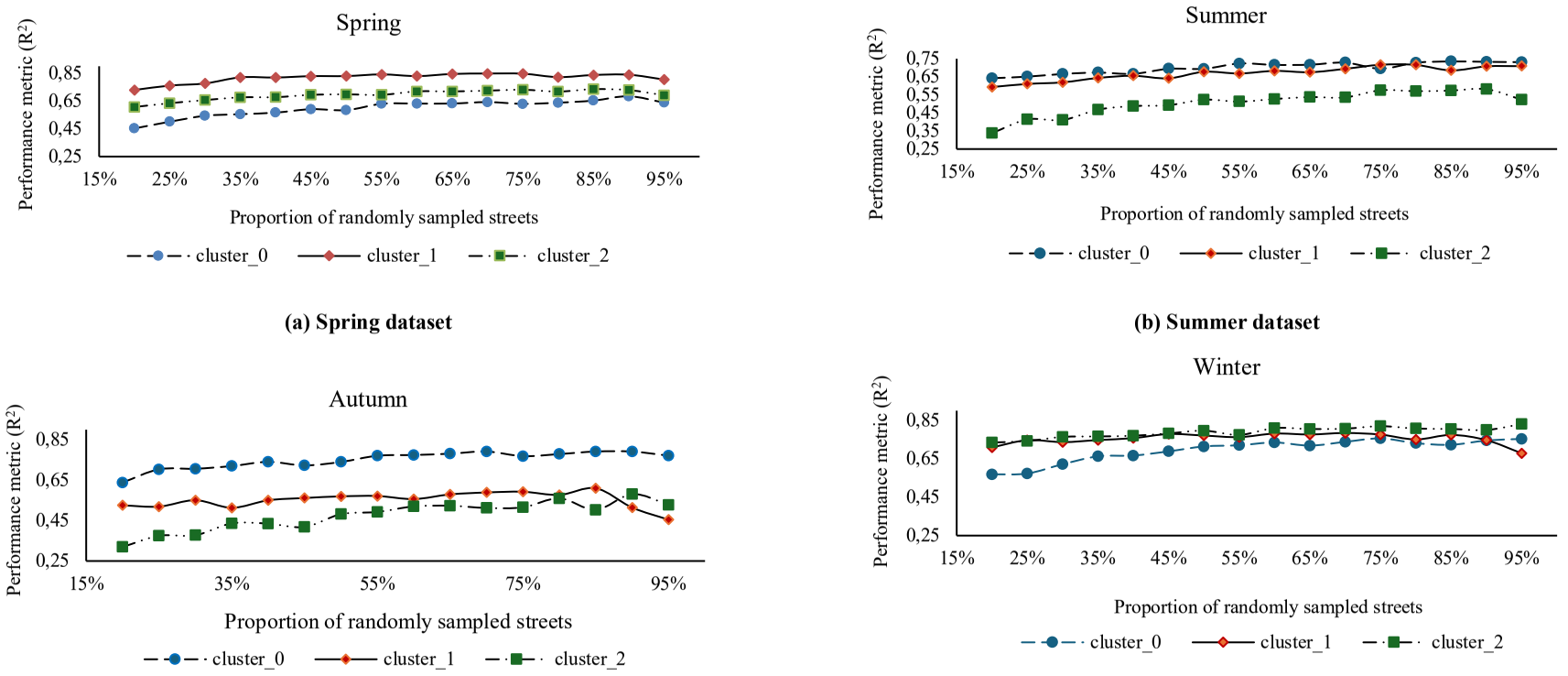

(a) Spring dataset **(b) Summer dataset**

(c) Autumn dataset **(d) Winter dataset**

Figure 3. Performance Metrics by Street Typology and Season. The x-axis denotes the proportion of the dataset that was utilized to train the models, where for instance, 15% indicates that 15% of the dataset was employed for model training. The y-axis shows the Coefficient of Determination (R^2) values obtained from each subset of data, reflecting the model's performance. For example, in the Autumn dataset, using 15% of the data for training resulted in R^2 values ranging from 0.25 to 0.65 across all clusters.

In summer (Fig. 3 (b) the R^2 values for clusters 0, 1, and 2 are very flat, indicating that sampling more streets does not significantly change the model's performance. Cluster_1, in particular, maintains a high R^2 value close to 0,85, suggesting robust model accuracy. Cluster_0 and cluster_2 are slightly worse, with very little variation across sample sizes. The flat performance across all clusters implies that for Summer, a minimal sample size might be just as effective as a larger one for capturing the behaviour of CUHI, and SUHI.

Regarding autumn, as shown in Fig. 3 (c) there is more variability, particularly for clusters 1 and 2, which both exhibit a downward trend in R^2 values as the proportion of sampled streets increases. This result suggests that including more data does not necessarily translate to greater accuracy and may even introduce noise, due to overfitting. This directly challenges the general idea that the more data the better. Conversely, cluster_0 demonstrates variability in the proportion of data samples needed to achieve the highest predictive performance. This suggests that the optimal data sample size varies and is influenced by both the season in question and the specific urban context of the study. The winter season (Fig. 3 (d)) shows distinct trends for each cluster. Cluster_0 shows an initial improvement in R^2 with an increase in sampled streets, suggesting that a certain threshold of data quantity can enhance model accuracy. This indicates that a sample size of about 35% could be ideal for cluster_0 in Winter. In contrast, clusters 1 and 2 both show a gradual decrease in R^2 values as more streets are sampled, implying that a smaller dataset might be more suitable for these clusters during the cold season to avoid a decline in predictive performance. The diverging trends across clusters underscore the necessity to tailor the sample size to the specific context, even at the street level.

3.3 Validation

The original dataset comprised 17,325 data instances and a total of 105 unique streets. When the model was trained using the entire dataset, the maximum accuracy was achieved in terms of R^2 of 0.82 for CUHI and 0.80 for SUHI. Based on the results from the previous section, the RF model was now trained per season using a sample of streets per cluster, Table 1, summarizes the total number of streets per cluster. To validate the hypothesis of the study, from these clusters, a percentage of data was selected to train the model per season. As summarized in Table 2, for the summer and spring seasons, 45% of the dataset was used to train the models. The results show that the CUHI model achieved an R^2 score of 0.84 in summer and 0.85 in spring, indicating a high level of accuracy in predicting outcomes based on the input variables. The SUHI model, on the other hand, showed a consistent R^2 score of 0.74 for both seasons, suggesting a slightly lower but still substantial predictive accuracy compared to CUHI. for autumn and winter seasons, where a larger percentage of the dataset was used for training, 65% for autumn and 75% for winter. The need for this increased dataset size might be attributed to the seasonal low variability and therefore the need to capture a broader range of infrastructure. The CUHI model continued to outperform the SUHI model in these seasons as well, with R^2 scores of 0.83 (autumn) and 0.93 (winter) for CUHI, and 0.72 (autumn) and 0.77 (winter).

4. Discussion

This study contributes to the broader debate on urban heat mitigation by emphasizing the critical role of seasonal dynamics, and the benefits of tailoring data collection methods. The seasonal analysis revealed that SUHI and CUHI intensities are pronounced during the summer and fade in the winter, aligning with expected temperature fluctuation patterns. As Schatz and Kucharik (2014) have discussed, this seasonal fluctuation highlights the significance of incorporating the temporal dimension into UHI studies to accurately assess and address the dynamic of UHI throughout the year. Furthermore, this research advances the field by quantifying the magnitude of these fluctuations at a granular, street-level resolution for both SUHI and CUHI. This not only highlights the complexity inherent in UHI phenomena but also stresses the need for simultaneous consideration of both CUHI and SUHI in research and urban planning strategies. To put it in context, in the spring for instance, the DTW distance for CUHI was markedly lower compared to SUHI, suggesting that SUHI experiences almost three times more variability. If urban heat mitigation strategies are predominantly based on air temperature measurements collected by weather stations, they might inadvertently prioritize CUHI dynamics. Such an approach risks underrepresenting the variability and intensity of SUHI, and ultimately rendering inadequate the mitigation measures.

	Summer	**Spring**	**Autumn**	**Winter**
Cluster_0	23	34	51	59
Cluster_1	33	21	25	19
Cluster_2	49	50	29	27

Table 1: Distribution of Street Clusters by Season. The table presents the total number of streets grouped into three distinct clusters (0, 1, and 2) for each season.

	% Dataset	Metric	CUHI	SUHI
Summer	45	R2	0,84	0,74
		MAE	0,23	1,21
Spring	45	R2	0,85	0,74
		MAE	0,26	0,96
Autumn	65	R2	0,83	0,72
		MAE	0,19	0,82
Winter	75	R2	0,93	0,77
		MAE	0,10	0,49

Table 2: Comparative seasonal performance of CUHI and SUHI models. The table summarizes the R^2 and MAE metrics reflecting the accuracy and error rates for CUHI and SUHI across four seasons, alongside the percentage of the dataset used for the models during each season.

5. Conclusions

By leveraging ML algorithms, this research introduces a methodology designed to optimize data collection efforts. This methodology shifts away from broad, indiscriminate data gathering towards a more focused collection of crucial data, specifically targeting street typologies that exhibit uniform UHI mechanisms. Demonstrating the effectiveness of this approach, the study effectively trained RF models using varying proportions of dataset sizes across different seasons: 45% for summer and spring, 65% for autumn, and 75% for winter. Despite the reduced size of the training dataset, the models achieved notable accuracies, with the CUHI model reaching an accuracy of 0.85 and the SUHI model achieving 0.74 in the predictive metrics. These results validate the hypothesis that a selective data collection strategy, informed by analysis of seasonal variations and street typology, can effectively capture the complex dynamics of UHI. Such a nuanced strategy does not

merely broaden our understanding of UHI. The dual advantage of this approach lies in its potential to minimize the resources allocated for data collection while concurrently increasing the accuracy and relevance of urban heat analysis, presenting cost-effective and precise modelling.

The methodology employed in this study showcased that utilizing a reduced dataset could still achieve high accuracy in modelling the mechanics of UHI based on street typologies. However, it is critical to acknowledge that the data collection was limited to a single city. For future research, incorporating data from a more diverse range of built environments is essential to enhance the robustness and applicability of the findings across different urban contexts. Additionally, the authors are currently exploring an intriguing research direction: the integration of physics-based and data-driven modelling. This approach implies that physics-based models, informed by data from collection campaigns, can simulate various scenarios. These simulations, in turn, could serve as valuable inputs for refining data-driven models, offering a synergistic framework that leverages both theoretical foundations and empirical insights to better understand and mitigate UHI.

References

Aghabozorgi, S., Shirkhorshidi, A.S., Wah, T.Y., 2015. Time-series clustering–a decade review. Information systems 53, 16-38.

Akbari, H., Cartalis, C., Kolokotsa, D., Muscio, A., Pisello, A.L., Rossi, F., Santamouris, M., Synnefa, A., Wong, N.H., Zinzi, M., 2016. Local climate change and urban heat island mitigation techniques – the state of the art. Journal of Civil Engineering and Management 22, 1-16.

Copernicus, E.U.S.E.O.P.-. 2023. The 2023 Annual Climate Summary: Global Climate Highlights 2023.

Du, H., Zhan, W., Liu, Z., Li, J., Li, L., Lai, J., Miao, S., Huang, F., Wang, C., Wang, C., Fu, H., Jiang, L., Hong, F., Jiang, S., 2021. Simultaneous investigation of surface and canopy urban heat islands over global cities. ISPRS Journal of Photogrammetry and Remote Sensing 181, 67-83.

Grimmond, C.S.B., Blackett, M., Best, M.J., Baik, J.J., Belcher, S., Beringer, J., Bohnenstengel, S., Calmet, I., Chen, F., Coutts, A., 2011. Initial results from Phase 2 of the international urban energy balance model comparison. International Journal of Climatology 31, 244-272.

Hu, Y., Hou, M., Jia, G., Zhao, C., Zhen, X., Xu, Y., 2019. Comparison of surface and canopy urban heat islands within megacities of eastern China. ISPRS Journal of Photogrammetry and Remote Sensing 156, 160-168.

Jandaghian, Z., Berardi, U., 2020. Comparing urban canopy models for microclimate simulations in Weather Research and Forecasting Models. Sustainable Cities and Society 55.

Mirzaei, P.A., Haghighat, F., 2010. Approaches to study urban heat island–abilities and limitations. Building and environment 45, 2192-2201.

Oke, T.R., 1982. The energetic basis of the urban heat island. Quarterly Journal of the Royal Meteorological Society 108, 1-24.

Pena Acosta, M., Dikkers, M., Vahdatikhaki, F., Santos, J., Dorée, A., 2023a. A comprehensive generalizability assessment of data-driven Urban Heat Island (UHI) models. Sustainable Cities and Society.

Pena Acosta, M., Vahdatikhak, F., Santos, J., Hammad, A., Doree, A., 2022. A framework for a comprehensive mobile data acquisition setting for the assessment of Urban Heat Island phenomenon, 39th International Symposium on Automation and Robotics in Construction, ISARC 2022.

Pena Acosta, M., Vahdatikhaki, F., Santos, J., Dorée, A., 2023b. A comparative analysis of surface and canopy layer urban heat island at the micro level using a data-driven approach. Sustainable Cities and Society.

Pena Acosta, M., Vahdatikhaki, F., Santos, J., Jarro, S.P., Dorée, A.G., 2024. Data-driven analysis of Urban Heat Island phenomenon based on street typology. Sustainable Cities and Society 101.

Peng, S., Piao, S., Ciais, P., Friedlingstein, P., Ottle, C., Bréon, F.-M., Nan, H., Zhou, L., Myneni, R.B., 2012. Surface urban heat island across 419 global big cities. Environmental science & technology 46, 696-703.

Peng, W., Wang, R., Duan, J., Gao, W., Fan, Z., 2022. Surface and canopy urban heat islands: Does urban morphology result in the spatiotemporal differences? Urban Climate 42.

Roßbach, P., 2018. Neural networks vs. random forests–does it always have to be deep learning. Germany: Frankfurt School of Finance and Management.

Sakoe, H., Chiba, S., 1978. Dynamic programming algorithm optimization for spoken word recognition. IEEE transactions on acoustics, speech, and signal processing 26, 43-49.

Schatz, J., Kucharik, C.J., 2014. Seasonality of the urban heat island effect in Madison, Wisconsin. Journal of Applied Meteorology and Climatology 53, 2371-2386.

Sheng, L., Tang, X., You, H., Gu, Q., Hu, H., 2017. Comparison of the urban heat island intensity quantified by using air temperature and Landsat land surface temperature in Hangzhou, China. Ecological Indicators 72, 738-746.

Sun, Y., Gao, C., Li, J., Wang, R., Liu, J., 2019. Quantifying the effects of urban form on land surface temperature in subtropical high-density urban areas using machine learning. Remote Sensing 11, 959.

Venter, Z.S., Chakraborty, T., Lee, X., 2021. Crowdsourced air temperatures contrast satellite measures of the urban heat island and its mechanisms. Science Advances 7, eabb9569.

Wang, R., Gao, W., Peng, W., 2020. Downscale MODIS land surface temperature based on three different models to analyze surface urban heat island: a case study of Hangzhou. Remote Sensing 12, 2134.

Witten, I.H., Frank, E., Hall, M.A., Pal, C.J., 2017. Data Mining: Practical Machine Learning Tools and Techniques. Elsevier.
Zhou, B., Rybski, D., Kropp, J.P., 2013. On the statistics of urban heat island intensity. Geophysical research letters 40, 5486-5491.